HHS Public Access

Author manuscript

Sci Signal. Author manuscript; available in PMC 2018 May 23.

Published in final edited form as:

Sci Signal. ; 10(480): . doi:10.1126/scisignal.aam7479.

Enzalutamide-induced "BRCAness" and PARP inhibition is a synthetic lethal therapy for castration-resistant prostate cancer

Likun Li[1], **Styliani Karanika**[1,†], **Guang Yang**[1], **Jiangxiang Wang**[1], **Sanghee Park**[1], **Bradley Broom**[2], **Ganiraju C. Manyam**[2], **Wenhui Wu**[2], **Yong Luo**[1], **Spyridon Basourakos**[1], **Jian H. Song**[1], **Gary E. Gallick**[1], **Theodoros Karantanos**[1,‡], **Dimitrios Korentzelos**[1], **Abul Kalam Azad**[1], **Jeri Kim**[1], **Paul G. Corn**[1], **Ana M. Aparicio**[1], **Christopher J. Logothesis**[1], **Particia Troncoso**[3], **Heffernan Timothy**[4], **Carlo Toniatti**[5], **Hyun-Sung Lee**[6], **Ju-Seog Lee**[6], **Xuemei Zuo**[1], **Wenjun Chang**[1,§], **Jianhua Yin**[1,§], and **Timothy C. Thompson**[1,*]

[1]Department of Genitourinary Medical Oncology, The University of Texas MD Anderson Cancer Center, 1515 Holcombe Blvd., Houston, TX 77030-4009

[2]Department of Bioinformatics and Computational Biology, The University of Texas MD Anderson Cancer Center, 1515 Holcombe Blvd., Houston, TX 77030-4009

[3]Department of Pathology, The University of Texas MD Anderson Cancer Center, 1515 Holcombe Blvd., Houston, TX 77030-4009

[4]Institute for Applied Cancer Science, The University of Texas MD Anderson Cancer Center, 1515 Holcombe Blvd., Houston, TX 77030-4009

[5]ORBIT (Oncology Research for Biologics and Immunotherapy Translation), The University of Texas MD Anderson Cancer Center, 1515 Holcombe Blvd., Houston, TX 77030-4009

[*]Corresponding author. timthomp@mdanderson.org.

[†]Current address: Infectious Diseases Division, Warren Alpert Medical School of Brown University, Rhode Island Hospital, 593 Eddy Street, POB, 3rd Floor, Suite 328/330, Providence, RI 02903;

[‡]Current address: General Internal Medicine Section, Boston Medical Center, Boston University School of Medicine, 840 Harrison Ave, Boston, MA 02118;

[§]Current address: Department of Epidemiology, The Second Military Medical University, Shanghai 200433, China.

Supplementary Materials

Fig. S1. Sequence and copy number variation analysis using the T200 platform

Fig. S2. Titration of ENZ and OLA in colony assays.

Table S1. Determination of synergy.

Table S2. Expression of pro-apoptotic genes.

Table S3. Expression of anti-apoptotic genes.

Table S4. Primers and probes for qRT-PCR.

Table S5. siRNA sources and sequences.

Author contributions: T.C.T. and L.L. conceived and designed the study and wrote the paper. : L.L., J.W., X.Z., W.C., and J.Y. cell performed the culture studies. S.K., S.P., J.W., Y.L., S.B., J.S., G.E.G., and T.K. performed the xenograft model experiments. G.Y., and D. K. performed the immunohistochemistry analysis. B.M.B., G.M., W.W., and A.K. A. performed the gene expression analysis of CRPC patient tissue samples and integrated genomic analysis of cell lines and xenograft models. J. K. P.G.C., A.M.A., and C.J.L. provided clinical insight and concept development. P.T. performed the pathology evaluation of human PCa samples.: J.-S.L. and HS. L. performed the microarray experiments. T.H. and C.T. provided intellectual contributions. G.E.G. revised the manuscript. All authors contributed to data analysis.

Competing interests: The authors declare they have no competing financial interests.

Data and materials availability: Microarray data are deposited in the Gene Expression Omnibus (http://www.ncbi.nlm.nih.gov/geo/), accession number GSE69249.

[6]Department of Systems Biology, The University of Texas MD Anderson Cancer Center, 1515 Holcombe Blvd., Houston, TX 77030-4009

Abstract

Cancers with dysfunctional mutations in *BRCA1* or *BRCA2*, most commonly associated with some breast cancers, are deficient in the DNA damage repair pathway called homologous recombination (HR), which makes them exquisitely vulnerable to poly(ADP-ribose) polymerase (PARP) inhibitors, such as olaparib. This functional state and therapeutic sensitivity is referred to as "BRCAness". Pharmaceutical induction of BRCAness could expand the use of PARP inhibitors to other tumor types. For example, *BRCA* mutations are present in only a small proportion of prostate cancer (PCa) patients. We found that castration-resistant PCa (CRPC) cells increased expression of a set of HR-associated genes, including *BRCA1*, *RAD54L* and *RMI2*. Androgen-targeted therapy is typically not effective in CRPC patients. However, the androgen receptor (AR) inhibitor enzalutamide suppressed the expression of those HR genes, thus creating HR deficiency and BRCAness in CRPC cells. In a manner dependent on these gene expression effects, a "lead-in" treatment strategy, in which enzalutamide was followed by the combination of enzalutamide and olaparib, promoted DNA damage-induced cell death and inhibited clonal proliferation of PCa cells in culture and suppressed the growth of PCa xenografts in mice. Thus, our study suggests that anti-androgen and PARP inhibitor combination therapy may be effective for patients with CRPC, and that pharmaceutically-induced BRCAness may expand the clinical use of PARP inhibitors.

Introduction

Metastatic prostate cancer (PCa) is incurable and the second-leading cause of cancer deaths among men in the western world (1). Although patients initially respond to androgen-deprivation therapy (ADT), most eventually develop castration-resistant prostate cancer (CRPC) and metastasis to bone, the predominant site of advanced, lethal PCa (2, 3). Abiraterone acetate (ABI) and enzalutamide (ENZ), novel androgen receptor (AR)-signaling inhibitors (4, 5), each extends the life of metastatic CRPC (mCRPC) patients for 4–5 months, but neither of these agents are curative. Therefore, more effective therapies are needed, including novel therapeutic combinations and innovative therapy sequencing approaches.

The development of CRPC is accompanied by the accumulation of gene mutations, chromosomal translocations, and enhanced DNA repair activities that enable CRPC cells to survive and proliferate (6–8). Moreover, increased expression of certain DNA repair genes reflects reduced DNA repair proficiency; and these activities are associated with greater mutagenesis, adverse clinical features and inferior patient survival rates (9). Poly(ADP-ribose) polymerase (PARP) inhibitors, which can abrogate base excision repair, or trap PARP on the DNA, are promising therapeutic agents that show synthetic lethality against many types of cancer with BRCA1 or BRCA2 deficiencies (10–13). Although a favorable response of cancers to PARP inhibition due to BRCA1 or BRCA2 mutations has been demonstrated, PARP inhibitors have not been widely used in cancers with deficiencies of other homologous recombination (HR) genes. Promising clinical studies using PARP inhibitors are underway (14– 16), and it is now essential to further our understanding of the

HR pathway to maximize the benefit of PARP inhibitor therapy for CRPC. BRCA germ line/somatic mutations/deletions account for only 12–20% of CRPC patients (6, 14, 17, 18); therefore, pharmaceutically-induced HR deficiency becomes an attractive and clinically viable strategy that potentially expands the benefit of PARP inhibitor therapy to CRPC patients who do not have BRCA mutations.

Accumulating evidence revealed the convergence of DNA damage response (DDR) signaling pathways and AR signaling pathways in PCa (8, 19–22). We previously found that an AR and c-Myb coregulated DDR gene signature is correlated with prostate cancer metastasis, castration resistance, tumor recurrence, and reduced survival in PCa patients (8). The presence of a relatively large number of HR genes in this AR- and c-Myb-coregulated DDR gene signature, together with the identification of a CRPC-upregulated HR gene signature (Fig. 1), led us to consider that pharmaceutically-induced downregulation of AR-regulated HR genes may induce HR deficiency, and sensitize CRPC to PARP inhibition. Therefore, targeting AR by ENZ and PARP by olaparib (OLA) would generate synthetic lethality in CRPC. Here, we report that ENZ downregulated a specific set of HR genes, including *BRCA1*, *RAD51AP1*, *RAD51C*, *RAD54L*, and *RMI2*, and this pharmaceutically-induced HR deficiency synergizes with the effects of OLA to induce DNA damage-related cell death, inhibit PCa cell clonal growth, and suppress xenograft tumor growth.

Results

Expression of HR-associated genes is upregulated in CRPC

To extend our previous study showing the correlation of advanced PCa and AR- and c-Myb-coregulated DDR gene signature, in which HR-associated genes are highly represented (8), we identified specific HR genes that were upregulated in CRPC using two public patient data sets (6, 17) and a Gene Ontology defined HR gene set (37 genes). Analysis of these HR genes showed significant differential expression between hormone naïve primary PCa and CRPC samples. Statistically altered HR genes were identified, after Benjamini–Hochberg correction for multiple hypotheses testing, $p < 0.05$, and those common to both datasets were identified (Fig. 1A-B). There were 10 upregulated HR genes common to both datasets, including *CHEK1, BRCA1, EXO1, BLM, RMI1, RAD54L, RAD51, LIG1, XRCC3* and *RMI2*, and 1 downregulated HR gene (*RPA1*). Analysis of gene expression in CRPC tissue samples revealed that a set of HR genes are overexpressed in CRPC and positively correlated with CRPC development and adverse clinical outcome (Figs. 1, C and D).

ENZ, OLA, and their combination inhibit HR-associated gene expression in AR-positive PCa cells

To test our hypothesis that pharmaceutically-induced downregulation of AR-regulated HR genes may induce BRCAness and sensitize CRPC to PARP inhibition, we examined the effect of ENZ, OLA, and the combination (ENZ+OLA) on HR gene expression in multiple PCa cell lines with variable androgen dependence. Microarray analysis revealed that expressions of 15 out of 37 HR genes were statistically altered in response to drug treatment (after Benjamini–Hochberg correction for multiple hypotheses testing, $p < 0.05$) (Fig. 2A). Among these 15 HR genes, we selected 5 genes, namely *BRCA1, RAD51AP1, RAD51C,*

RAD54L and *RMI2* for further investigation. Our selections were made on the basis of the following: *BRCA1*, *RAD54L* and *RMI2* are among the 10 upregulated HR genes in CRPC in both of the independent clinical datasets (Fig. 1); these 5 genes are among most significantly altered ENZ-targeted, downregulated HR genes; and these 5 genes are involved in different critical steps in HR-mediated DNA repair (23–26). qRT-PCR (Fig. 2B-D) and Western blotting (Fig. 2E) analyses showed that ENZ treatment inhibited the expression of all 5 genes in VCaP cells (AR-positive; the most androgen-dependent of the three cell lines used; derived from a vertebral metastatic lesion of a patient with hormone refractory prostate cancer), and inhibited all 5 genes to a lesser extent in LNCaP cells (AR-positive but less androgen-dependent than VCaP; derived from a supraclavicular lymph node metastatic lesion from a patient with hormone refractory prostate cancer), but did not inhibit any of these genes in CWR22Rv1 cells (AR-positive and androgen-independent; derived from a primary prostate tumor that expresses mutant (H874Y) androgen receptors (AR) and secretes low amounts of prostate specific antigen). Unexpectedly, OLA treatment suppressed the expression of the majority of these HR genes in LNCaP cells and all of these HR genes in CWR22Rv1 cells, but had very little effect on these HR genes in VCaP cells. Further downregulation of these HR genes by the combination of ENZ and OLA compared to single agent alone was evident in the LNCaP model (Fig. 2A-E).

HR genes cooperatively contribute to DNA repair and PCa cell survival

To determine the role of these ENZ-downregulated HR genes with regard to OLA sensitivity of PCa cells, we performed cell-cycle analysis to quantitate sub-G1 (apoptotic) cells resulting from HR gene silencing and OLA combination treatment. We screened multiple siRNAs for each HR gene using VCaP cells, selected two most effective siRNAs for each HR gene to analyze the biological activities in VCaP cells, and then chose the more effective one to use for the analysis in LNCaP and CWR22Rv1 cells. Our results demonstrate that each HR gene differentially contributes to resistance to OLA treatment and PCa cell survival as indicated by the increase in the sub-G1 cell population in response to knockdown of a specific HR gene (Fig. 3A-F). Synergy analyses using two-way ANOVA (27) and Bliss independence model (28) indicated that knockdown of BRCA1, RAD51C, or RMI2 synergized with OLA in all three cell lines; knockdown of RAD51AP1 synergized with OLA in VCaP and CWR22Rv1 cells; and knockdown of RAD54L synergized with OLA in LNCaP and CWR22Rv1 cells (Fig. 3D-F; table S1).

HR is a multi-step biological process (23–26). We hypothesized that ENZ- and/or OLA-downregulated HR genes that function at different HR steps cooperatively contribute to DNA repair and PCa cell survival. Therefore, simultaneous knockdown of multiple HR genes should cooperatively enhance the HR deficiency phenotype and synergize the HR defect with OLA. We selected *BRCA1*, *RAD51C*, and *RMI2* to test cooperative functions because these three HR genes are involved in the recruitment of early HR factors to DSBs, formation of the RAD51 nucleoprotein filaments, and resolution of Double Holiday Junctions (DHJ), respectively (23–26), and because the siRNAs for each of these three HR genes showed synergy with OLA treatment in all three cell lines tested (Fig. 3D-F). Simultaneous knockdown of two or three HR-associated genes markedly increased the abundance of γH2AX protein (a marker of DNA damage) and cleaved PARP (a marker of

apoptosis) (Fig. 3G), significantly increased proportion of sub-G1 cells (Fig. 3H), and significantly reduced capacity for colony formation (Fig. 3I) compared with knockdown of each HR gene singly. Synergistic effects were observed in the majority of HR-associated siRNA combinations and HR-associated siRNA and OLA combinations (Fig. 3H-I, and table S1). Dual knockdown of BRCA1 and RMI2 showed the greatest effects (Fig. 3G-I) among the tested dual siRNA combinations. Together, these results suggest that ENZ-regulated HR genes cooperatively contribute to DNA repair and PCa cell survival.

ENZ and/or OLA inhibits HR efficiency

γH2aX and RAD51 are two markers of DNA damage, DNA repair and treatment sensitivity in preclinical and clinical samples (29). To determine whether ENZ and OLA treatment leads to reduced HR efficiency, we conducted double immunofluorescence staining to assess the formation of γH2aX and RAD51 foci and their colocalization in OLA+ENZ-treated LNCaP cells (Fig. 4A). Quantitative analyses demonstrated that the percentages of cells that contain γH2AX foci was significantly higher in ENZ+OLA-treated cells compared to OLA-treated cells (Fig. 4B, **left**), and the percentage of cells with both γH2AX and RAD51 foci was significantly lower in response to ENZ+OLA treatment than to OLA treatment alone (Fig. 4B, **right**). Foci ratio of RAD51 to γH2AX was significantly lower in ENZ+OLA-treated cells than in those treated with OLA alone (Fig. 4C). Analysis of drug-treated LNCaP cells using a qPCR-based HR assay showed that ENZ and OLA each reduced HR efficiency, and that their combination further reduced HR efficiency (Fig. 4D). Western blotting analysis of drug-treated LNCaP cells indicated that combination ENZ+OLA treatment markedly increased DNA damage or its persistence (γH2AX) and DNA damage-induced apoptosis (cleaved PARP) (Fig. 4E). Together, these data suggest that the cytotoxic effects of the ENZ+OLA combination is mediated by deficient DNA repair.

Lead-in ENZ+OLA strategy synergistically increases apoptosis and inhibits clonogenic growth in PCa cells

To optimize treatment conditions of ENZ and OLA combination, we compared a lead-in ENZ+OLA treatment strategy with a traditional concomitant ENZ+OLA strategy. In the lead-in ENZ+OLA treatment, we pretreated PCa cells with ENZ for 24 hours (lead-in time), then with ENZ+OLA for 48 hours. This protocol achieved ENZ-mediated downregulation of HR genes before OLA was applied. In the concomitant ENZ+OLA treatment, cells were treated with DMSO (vehicle control for ENZ) for 24 h, and then with ENZ+OLA for 48 h. The resulting data showed that the lead-in ENZ+OLA treatment increased sub-G1 cells and inhibited colony growth more effectively than traditional concomitant ENZ+OLA treatment in VCaP and LNCaP cells (AR-positive, androgen-dependent), but not in CWR22Rv1 cells (AR-positive, androgen-independent) (Figs. 5A-D and table S1).

Because the lead-in ENZ+OLA treatment protocol further increased the number of apoptotic cells compared to the concomitant ENZ+OLA protocol, we considered differential ENZ versus OLA apoptotic activities combined with increased exposure to ENZ during the lead-in treatment phase as underlying, cooperative mechanisms for the lead-in effect. Using unambiguous pro- and anti-apoptotic gene subsets derived from the Gene Ontology-defined apoptosis gene set (GO: 0006915), we pooled microarray expression data of these pro- and

anti-apoptotic genes, adjusted p-value using Benjamini–Hochberg procedure for multiple hypotheses testing, and identified statistically significant ($p<0.05$) alterations in gene expression in ENZ, OLA or lead-in ENZ+OLA treated samples compared to those treated with vehicle (tables S1 and S2). In addition to overlapping subsets of ENZ- and OLA-induced upregulated pro-apoptotic genes and overlapping subsets of ENZ- and OLA-induced downregulated anti-apoptotic genes, which could contribute to synergistic effects from ENZ and OLA, we found that two of the anti-apoptotic genes, serum/glucocorticoid regulated kinase 1 (*SGK1*) and TNF alpha induced protein 8 (*TNFAIP8*), were downregulated by ENZ but upregulated by OLA, which led us to speculate that the lead-in protocol would enable maximal ENZ-induced suppression, and delay OLA upregulation of these specific anti-apoptotic genes. Both SGK1 and TNFAIP8 reportedly participate in apoptosis evasion, cell survival, chemo resistance and tumor progression (Fig. 5E) (30–33) (34). Western blotting analysis validated select ENZ- and OLA-upregulated pro-apoptotic genes and ENZ-downregulated and OLA-upregulated *SGK1* and *TNFAIP8* (Fig. 5F). To validate the pro-cell survival roles of SGK1 and TNFAIP8, we knocked down each in LNCaP cells (Fig. 5G) and performed cell cycle analysis to assess sub-G1 cell distribution. SGK1 knockdown alone caused only a slight increase in the proportion of sub-G1 cells but significantly increased the proportion of sub-G1 cells when combined with OLA, whereas TNFAIP8 knockdown alone significantly increased the proportion of sub-G1 cells that was further increased by combination with OLA (Fig. 5H). Our data suggest that in addition to downregulation of specific HR genes, downregulation of *SGK1* and *TNFAIP8* expression by ENZ prior to OLA treatment, in part, contributes to the superior therapeutic effect of the lead-in ENZ+OLA strategy.

Lead-in ENZ+OLA treatment strategy synergistically suppresses PCa growth

To test our finding of synergism in the lead-in ENZ+OLA treatment strategy in vivo, we analyzed ENZ or OLA alone and concomitant or lead-in combination ENZ+OLA treatment using a subcutaneous patient-derived xenograft (PDX) tumor model [MDA PCa 133-4, AR-positive, implanted in pre-castrated severe combined immunodeficiency (SCID) mice], and two orthotopic PCa cell line xenograft models (VCaP, AR-positive, androgen-dependent; CWR22Rv1, ARpositive, androgen-independent) (Fig. 6A). In the MDA 133-4 subcutaneous model, treatment with ENZ or OLA alone was sufficient to suppress tumor growth, indicated by reduced tumor volumes (Fig. 6B) and tumor weights (Fig. 6C), with ENZ demonstrating superior efficacy among the two single agents. The in vivo lead-in treatment with ENZ+OLA, which mimicked that used in cultured cells, achieved significantly greater tumor suppression than treatment with either OLA or ENZ alone or with concomitant ENZ+OLA treatment (Fig. 6B–C). Synergy analysis revealed a synergistic therapeutic effect in the lead-in ENZ+OLA group (Fig. 6B–C and table S1). Analysis of xenograft tumor samples demonstrated significantly reduced BRCA1 protein abundance and Ki67 staining in tumors from mice treated with the lead-in ENZ+OLA protocol compared to those from mice treated with vehicle, ENZ or OLA alone, or concomitant ENZ+OLA (Fig. 6D–E). Similar results were observed using VCaP orthotopic xenograft model (Fig. 7). ENZ had superior efficacy in the MDA 133-4 and VCaP models; by contrast, in the CWR22Rv1 model, OLA showed superior efficacy and the lead-in ENZ+OLA and concomitant ENZ +OLA showed efficacy similar to that of OLA alone (Fig. 8A–C). Whereas BRCA1

abundance was relatively unchanged (Fig. 8D), Ki67 labeling was significantly reduced in CWR22Rv1 xenograft samples from OLA- or lead-in ENZ+OLA-treated mice (Fig. 8E).

Discussion

The utilization of PARP inhibitors such as OLA has rapidly evolved from in vitro studies to clinical applications (16, 36, 37). However, only recently has limited information become available for PCa. Recent reports include the results from preclinical models (8, 38), a phase I clinical trial using OLA as single agent (15), a phase I/II clinical trial using veliparib in combination with temozolomide (39, 40), and a more recent phase 2 trial using OLA (14). It is noteworthy that Mateo *et al.* extended the BRCAness concept to mutations/deletions of genes involved in HR regulation (*ATM*), HR factor nuclear localization (*PALB2*), and chromatin remodeling during HR DNA repair (*HDAC2*), which conceptually supports our finding that *BRCA1/2* and other HR genes involved in different stages of HR DNA repair cooperatively contribute to OLA sensitivity and our proposal that pharmaceutically induced HR deficiency as a therapy concept for future clinical applications of OLA. By demonstrating that 10 specific HR genes are upregulated in CRPC in two public datasets, and that these upregulated HR gene represent therapy targets for ENZ+OLA combination treatment, we introduce a specific biomarker panel for the use of PARP inhibitors and expand the concept of BRCAness to the concept of HR deficiency for CRPC as regard to clinical applications of PARP inhibitors for synthetic lethal therapy.

HR occurs through a series of steps (23, 25, 26), and the five ENZ-downregulated HR genes we identified are involved in almost all the major steps. Our data suggest that each ENZ-downregulated HR gene has a role in HR and the maintenance of PCa cell survival, but that *BRCA1*, *RAD51C*, and *RMI2* in particular cooperatively contribute to DNA repair and PCa cell survival, perhaps through their roles sequential steps in the HR pathway. The superior performance of dual and triple knockdown underscores redundancy among HR mediators that may oppose PARP inhibitor efficacy. Therefore, ENZ-induced suppression of multiple HR genes is a viable strategy to improve the efficacy of PARP inhibitors. The concept, if applied clinically, may extend the benefit of PARP inhibition therapy to CRPC patients who do not bear germ line/somatic mutation/deletion of *BRCA1/2*, or other HR genes.

We also demonstrated that lead-in ENZ+OLA has a clear advantage compared to concomitant ENZ+OLA. In addition to downregulation of a specific set of HR genes by ENZ prior to OLA treatment, this strategy also allows maximal ENZ suppression of and delay of OLA upregulation of specific anti-apoptotic genes. SGK1 and TNFAIP8 are two ENZ-downregulated and OLA upregulated anti-apoptotic genes identified in this study and knockdown of either gene was proved to have significant synergistic effect with PARP inhibition as regard to apoptotic cell death. These results suggest that downregulation of SGK1 and TNFAIP8 by ENZ prior to OLA treatment is, at least, one of the mechanisms underlying the superior effect of lead-in ENZ+OLA over concomitant ENZ+OLA; they are also consistent with growing evidence that links SGK1 and TNFAIP8 to cancer cell survival, metastasis and chemo- and radio-resistance (30–34).

The results of our xenograft studies provided particularly compelling support for the clinical utility of the ENZ+OLA combination treatment approach for advanced PCa or CRPC. Synergistic growth suppression was associated with ENZ-sensitive models (i.e., MDA PCa133-4 and VCaP). The lead-in approach demonstrated clear superiority of the ENZ +OLA combination treatments for the ENZ-sensitive models compared to the traditional concomitant application protocols. Suppression of nuclear *BRCA1* levels by the ENZ+OLA combination was associated with treatment efficacy in these models. Overall, these results have direct relevance for future ENZ+OLA clinical trials, which should be considered in light of our results.

Our data also showed that OLA strongly suppressed HR genes in androgen-independent CWR22Rv1 cells, indicating a cell context-dependent role for OLA in HR gene regulation, and it is noteworthy that our results suggest a transition from AR-dependent to PARP-dependent regulation of HR genes. Future studies are warranted to address these possibilities. Although ENZ failed to synergize with OLA in this cell-line model, OLA can downregulate HR genes in this type of PCa cells and compensate for the loss of ENZ effect.

Overall, our study provides new insights into the molecular functions of ENZ, adds mechanistic rationale to the ENZ+OLA combination therapy, and underscores the importance of an expanded BRCAness concept in future clinical usage of OLA. More importantly, our findings support a randomized clinical trial for OLA as single agent or in combination with other agents in unselected patients with CRPC. Future investigations using baseline and OLA-treated patient tissue samples are warranted to link the genomic and transcriptomic landscape, including these ENZ-downregulated HR genes, with patient response to OLA therapy.

Materials and Methods

Sources of cell lines and PDXs

VCaP and LNCaP (American Type Culture Collection), and CWR22Rv1 (from Dr. Francis M. Sirotnak of Memorial Sloan-Kettering Cancer Center) cell lines were validated by short tandem repeat DNA fingerprinting with the AmpFℓSTR Identifiler PCR Amplification Kit (Applied Biosystems) in MD Anderson's Characterized Cell Line Core Facility. Genetic background (genomic alterations and copy number variations) of these cell lines, VCaP-luc, CWR22Rv1-luc and MDA 133-4 PDX model was analyzed using MDA T200 platform and summarized in fig. S1.

Gene expression microarray

cDNA microarray was performed using Illumina TotalPrep RNA Amplication Kit (ThermoScientific) and Ilumina Human T-12 v4.0 Expression BeadChip Kit (Illumina). Microarray data were deposited in the GEO database (accession number GSE69249).

Bioinformatics and biostatistics analyses

Grasso et. al.'s samples (GSE35988) were profiled on two different Agilent Whole Genome Microarrays. The two expression matrices (GPL6480 and GPL6848) were combined for

bioinformatics/biostatistics analyses, because no obvious batch effect was detected by Principal Component Analysis. Tylor et. al.'s samples (GSE21034) were profiled on Affymetrix Human Exon 1.0 ST arrays and transcript level expression matrix (GPL10264) was used for the analyses. The transcript accession numbers were converted to gene symbols using UCSC refGene annotation file and median expression level was used for genes with multiple transcripts. To compare the expression of 37 HR genes between normal prostate, hormone naïve PCa and CRPC samples, a linear model was fit to each of the genes, followed by Tukey's all-pair comparisons of the independent variable using R package 'multcomp'. The overall p-values were adjusted by Benjamini–Hochberg procedure. Genes with significant overall p-value (< 0.05) and also with significant p-value when comparing CRPC to either hormone naïve PCa or to normal prostate samples were selected from both Grasso and Tylor datasets. The common significantly upregulated and downregulated genes were used for box plots (Fig. 1A and Fig. 1B). The expression profile of the 10 commonly upregulated genes in Grasso et. al.'s (Fig. 1C) and Tylor et. al.'s (Fig. 1D) samples were shown in Semi-supervised hierarchical clustering heat maps. A similar statistical analysis was performed in cell line microarray data. The mean expression level was used for genes with multiple probes. The expression profile of genes with significant overall p-value and also significant p-value when comparing ENZ+OLA to DMSO for any of the three cell lines were shown in supervised hierarchical clustering heat map (Fig. 2A). Genes associated with apoptosis were obtained by the Gene Ontology term "Apoptosis" (GO: 0006915) and manually curated to characterize the Pro-Apoptosis and Anti-Apoptosis gene sets based on PubMed gene descriptions. Difference of gene expression across various treatments was assessed using ANOVA in these gene sets. The p-values were adjusted for multiple testing by Benjamini- Hochberg (FDR) method. Genes with adjusted p-values less than 0.05 are defined as significant. Further, Tukey's test is used to perform multiple comparison assessment with all the contrasts of interest in the dataset.

qRT-PCR

Total RNA from cancer cell lines was extracted with the RiboPure RNA extraction kit (Thermo Fisher Scientific). Reverse transcription (RT) reactions were carried out with the high-capacity cDNA archive kit (Applied Biosystem) according to the manufacturer's protocol. Real-time PCR was performed using the ABI PRISM 7000 sequence detection system (Applied Biosystems) according to the manufacturer's instructions. The relative quantity of mRNA was determined by the $\Delta\Delta C_T$ method as described by the manufacturer and normalized to GAPDH RNA in the same cDNA preparation. Primers and probes used for qRT-PCR were purchased from Integrated DNA Technologies (IDT) and are listed in table S4.

Immunohistochemical analysis

Antibodies to BRCA1 (ABCAM M110) and Ki67 (Santa Cruz SC15401) were used for immunostaining on formalin-fixed, paraffin-embedded tissue slides from the mouse PCa xenografts. Briefly, rehydrated slides were microwave-heated for 20 minutes in citrate buffer (10-mM, pH 6.0) for antigen retrieval. They were then incubated in 1% H_2O_2 for 10 minutes to inactivate endogenous horseradish peroxidase. After blocking with serum-free protein block (Dako X0909), they were incubated with the primary antibodies (BRCA1, 1: 100;

Ki67, 1: 100) for 90 minutes at room temperature, followed by incubation with HPR-conjugated secondary antibody (Dako K4061) for 40 minutes at room temperature. The immunoreaction products were visualized with 3, 3-diaminobenzidine (DAB)/H_2O_2 solution. For quantitative analyses, 15- 20 microscopic fields (at 200×) from each specimen were randomly selected and immunostaining results were evaluated by investigators (G.Y. and D.K.) who were blinded to the treatment information of a specimen and the nuclear BRCA1 or Ki67 labeling rates were recorded.

Lead-in ENZ+OLA treatment in cultured cells

VCaP, LNCaP, and CWR22Rv1 cells were pretreated with 1 μM ENZ or DMSO vehicle control for 24 hours, followed by treatment with ENZ (1 μM), OLA (10 μM for VCaP and LNCaP and 5 μM for CWR22Rv1), ENZ+OLA, or DMSO for 48 hours. The selection of OLA concentrations was based on the sensitivity of PCa cell lines to OLA.

Western blotting

Proteins were separated by electrophoresis using 4–20% gradient Mini_PROTEAN TGX Gels (Bio-Rad) and transferred onto nitrocellulose blotting membrane (GE Healthcare Life Sciences). Blots with interested proteins were blocked with TBS buffer containing 0.1% Tween 20 and 5% non-fat milk for 1 h and incubated with specific primary antibody overnight in a cold room rocker. After incubation with horseradish peroxidase (HRP) conjugated secondary antibody, blots were incubated with SuperSignal West Dura Extended Duration Substrate (Thermo Scientific) for 2 minutes and imaged with ChemiDoc MD Imaging System (Bio-Rad). Antibodies against BRCA1 (1: 2000), RAD51AP1 (1: 200), RAD51C (1: 200), RAD54 (1: 200), RMI2 (1: 2000), and TNFAIP8 (1: 500)were purchased from Abcam. Antibodies against γ- H2AX (1: 250), cleaved PARP (1: 500), SGK1 (1: 250) and GAPDH (1: 10000) were purchased from Cell Signaling Technology.

HR assay

HR assays were performed using LNCaP cells and an HR Assay Kit (Norgen Biotech) according to manufactuer suggested protocol. Briefly, LNCaP cells were transfected with dl-1 and dl-2 vectors that carried a mutated lacZ gene in each plasmid using FuGene transfection agent (Roche). After 6 h of plasmid transfection, cells were pretreated with ENZ or DMSO vehicle control for 18 h, followed by treatment with DMSO, ENZ, OLA, or ENZ +OLA for 24 h. Total DNA was isolated and qPCR analysis was performed using universal primers (for internal normalization) and assay-specific primers. The PCR cycle numbers for each sample using assay-specific primers was first normalized with respect to that in each sample using universal primers and then normalized with respect to control (control=1).

RNA interference

Cells were seeded one day prior to siRNA transfection (6–well format (for RNA or protein preparation): VCaP, 1×10^6/well, LNCaP, 5×10^5/well, CWR22Rv1, 2×10^5/well; 24-well format (for cell cycle analysis): 1/5 of cell numbers of 6-well format). SiRNA transfection was performed with 20 nM siRNA using RNAiMAX (Life Technology) according to the manufacturer's protocol. The sources and sequences of siRNAs are listed in table S5.

Flow cytometry analysis

Flow cytometry analysis was performed as described previously (8). Cells were seeded onto 24- well plates one day prior to the drug treatment or siRNA transfection. Flow cytometry analysis was performed 48 h after the drug treatment or siRNA transfection. In the case of siRNA and drug combination, siRNA transfection was performed one day prior to the drug treatment and flow cytometry analysis was performed 48 h after the drug treatment. Cells were harvested and prepared as a single cell suspension, washed with PBS, incubated with a staining buffer containing 0.1% sodium citrate, 0.1% Triton X-100 and 50 mg/ml propidium iodine for 30 min at 4°C, and proceeded to cell cycle analysis with FACS Canto II flow cytometer (BD Biosciences). Cell cycle profiles and quantitative data were obtained using FlowJo software (Tree Star Inc.).

Clonogenic assay

PCa cells were seeded at a low density in 6-well plates (VCaP, 1×10^5/well; LNCaP, 2×10^4/well; CWR22Rv1, 5×10^3/well), grown in normal growth medium for 10–20 days, and colonies were stained with 0.5% crystal violet and counted as described previously (8). Experiments were performed in triplicate and data were mean ±SD of three or more independent experiments.

Xenograft tumor assays

For the MDA 133-4 PDX model, equal-sized tumor pieces were implanted into subcutaneous pockets in the flanks of 6- to 8-week-old male CB17 SCID mice (Charles River Laboratories International, Inc., Wilmington, MA). VCaP cells (3×10^6) and CWR22Rv1 cells (2×10^6) were injected orthotopically into the prostates. When tumors reached an approximate volume of 30 mm^3, tumor-bearing mice were randomly placed in experimental subgroups to receive ENZ, OLA, ENZ+OLA (concomitant or lead-in: four-day pretreatment of ENZ before combined treatment with ENZ+OLA), or a vehicle control. ENZ, 10 mg/kg everyday orally, OLA, 40 mg/kg/day, 5 days each week, intraperitoneally. Subcutaneous tumor growth was monitored twice per week by caliper measurement, and orthotopic tumor growth was monitored weekly by bioluminescent images. Mice were sacrificed and tumor wet weights were determined. A subset of mice was euthanized, tumor specimens were collected, and formalin-fixed, paraffin-embedded tissue slides were prepared for immunohistochemical analysis of BRCA1 and Ki67 from tumors taken before or after 8–14 days of treatment.

Statistical analysis

ANOVA was used to assess difference of gene expression and Benjamini–Hochberg correction for multiple hypotheses testing was used to adjust the p-values in the determination of statistically altered HR genes in human PCa patient samples and in drug-treated PCa cell line samples; and statistically altered pro- or anti-apoptotic genes in drug-treated PCa cell line samples. Wilcoxon-Mann-Whitney test was used for data with non-normal distributions or data with small sample sizes, including qRT-PCR, cell cycle analysis, colony assay, and immunohistochemical analyses. ANOVA *t*-test was used for analysis of

tumor growth and tumor wet weights. Synergistic effects were determined by two-way ANOVA tests (27) and by the Bliss independence model (28).

Supplementary Material

Refer to Web version on PubMed Central for supplementary material.

Acknowledgments

Funding: This work was supported in part by the National Cancer Institute grant R0150588 (to T.C.T.); National Cancer Institute grant 5P50 CA140388, the Prostate Cancer Specialized Program of Research Excellence at The University of Texas MD Anderson Cancer Center; and the National Cancer Institute supported Grant CA16672, MD Anderson Cancer Center Support Grant. G.M. is supported by a grant from the Michael and Susan Dell Foundation.

References and Notes

1. Siegel R, Naishadham D, Jemal A. Cancer Statistics. CA Cancer J Clin. 2012; 62:10–29. [PubMed: 22237781]
2. Loblaw DA, Virgo KS, Nam R, Somerfield MR, Ben-Josef E, Mendelson DS, Middleton R, Sharp SA, Smith TJ, Talcott J, Taplin M, Vogelzang NJ, Wade JL 3rd, Bennett CL, Scher HI. Initial hormonal management of androgen-sensitive metastatic, recurrent, or progressive prostate cancer: 2006 update of an American Society of Clinical Oncology practice guideline. J Clin Oncol. 2007; 25:1596–1605. [PubMed: 17404365]
3. Sturge J, Caley MP, Waxman J. Bone metastasis in prostate cancer: emerging therapeutic strategies. Nat Rev Clin Oncol. 2011; 8:357–368. [PubMed: 21556025]
4. Derleth CL, Yu EY. Targeted therapy in the treatment of castration-resistant prostate cancer. Oncology (Williston Park). 2013; 27:620–628. [PubMed: 23977754]
5. Vogelzang NJ. Two paths forward in metastatic castration-resistant prostate cancer. Oncology (Williston Park). 2013; 27:638–639. [PubMed: 23977756]
6. Grasso CS, Wu YM, Robinson DR, Cao X, Dhanasekaran SM, Khan AP, Quist MJ, Jing X, Lonigro RJ, Brenner JC, Asangani IA, Ateeq B, Chun SY, Siddiqui J, Sam L, Anstett M, Mehra R, Prensner JR, Palanisamy N, Ryslik GA, Vandin F, Raphael BJ, Kunju LP, Rhodes DR, Pienta KJ, Chinnaiyan AM, Tomlins SA. The mutational landscape of lethal castration-resistant prostate cancer. Nature. 2012; 487:239–243. [PubMed: 22722839]
7. Baca SC, Prandi D, Lawrence MS, Mosquera JM, Romanel A, Drier Y, Park K, Kitabayashi N, MacDonald TY, Ghandi M, Van Allen E, Kryukov GV, Sboner A, Theurillat JP, Soong TD, Nickerson E, Auclair D, Tewari A, Beltran H, Onofrio RC, Boysen G, Guiducci C, Barbieri CE, Cibulskis K, Sivachenko A, Carter SL, Saksena G, Voet D, Ramos AH, Winckler W, Cipicchio M, Ardlie K, Kantoff PW, Berger MF, Gabriel SB, Golub TR, Meyerson M, Lander ES, Elemento O, Getz G, Demichelis F, Rubin MA, Garraway LA. Punctuated evolution of prostate cancer genomes. Cell. 2013; 153:666–677. [PubMed: 23622249]
8. Li L, Chang W, Yang G, Ren C, Park S, Karantanos T, Karanika S, Wang J, Yin J, Shah PK, Takahiro H, Dobashi M, Zhang W, Efstathiou E, Maity SN, Aparicio AM, Li Ning Tapia EM, Troncoso P, Broom B, Xiao L, Lee HS, Lee JS, Corn PG, Navone N, Thompson TC. Targeting poly(ADP-ribose) polymerase and the c-Myb-regulated DNA damage response pathway in castration-resistant prostate cancer. Sci Signal. 2014; 7:ra47. [PubMed: 24847116]
9. Pitroda SP, Pashtan IM, Logan HL, Budke B, Darga TE, Weichselbaum RR, Connell PP. DNA repair pathway gene expression score correlates with repair proficiency and tumor sensitivity to chemotherapy. Science translational medicine. 2014; 6:229ra242.
10. Ellisen LW. PARP inhibitors in cancer therapy: promise, progress, and puzzles. Cancer Cell. 2011; 19:165–167. [PubMed: 21316599]
11. Lord CJ, Ashworth A. The DNA damage response and cancer therapy. Nature. 2012; 481:287–294. [PubMed: 22258607]

12. Shen Y, Aoyagi-Scharber M, Wang B. Trapping Poly(ADP-Ribose) Polymerase. The Journal of pharmacology and experimental therapeutics. 2015; 353:446–457. [PubMed: 25758918]
13. Castro E, Mateo J, Olmos D, de Bono JS. Targeting DNA Repair: The Role of PARP Inhibition in the Treatment of Castration-Resistant Prostate Cancer. Cancer journal. 2016; 22:353–356.
14. Mateo J, Carreira S, Sandhu S, Miranda S, Mossop H, Perez-Lopez R, Nava Rodrigues D, Robinson D, Omlin A, Tunariu N, Boysen G, Porta N, Flohr P, Gillman A, Figueiredo I, Paulding C, Seed G, Jain S, Ralph C, Protheroe A, Hussain S, Jones R, Elliott T, McGovern U, Bianchini D, Goodall J, Zafeiriou Z, Williamson CT, Ferraldeschi R, Riisnaes R, Ebbs B, Fowler G, Roda D, Yuan W, Wu YM, Cao X, Brough R, Pemberton H, A'Hern R, Swain A, Kunju LP, Eeles R, Attard G, Lord CJ, Ashworth A, Rubin MA, Knudsen KE, Feng FY, 23 Chinnaiyan AM, Hall E, de Bono JS. DNA-Repair Defects and Olaparib in Metastatic Prostate Cancer. N Engl J Med. 2015; 373:1697–1708. [PubMed: 26510020]
15. Sandhu SK, Schelman WR, Wilding G, Moreno V, Baird RD, Miranda S, Hylands L, Riisnaes R, Forster M, Omlin A, Kreischer N, Thway K, Gevensleben H, Sun L, Loughney J, Chatterjee M, Toniatti C, Carpenter CL, Iannone R, Kaye SB, de Bono JS, Wenham RM. The poly(ADP-ribose) polymerase inhibitor niraparib (MK4827) in BRCA mutation carriers and patients with sporadic cancer: a phase 1 dose-escalation trial. Lancet Oncol. 2013; 14:882–892. [PubMed: 23810788]
16. Scott CL, Swisher EM, Kaufmann SH. Poly (adp-ribose) polymerase inhibitors: recent advances and future development. J Clin Oncol. 2015; 33:1397–1406. [PubMed: 25779564]
17. Taylor BS, Schultz N, Hieronymus H, Gopalan A, Xiao Y, Carver BS, Arora VK, Kaushik P, Cerami E, Reva B, Antipin Y, Mitsiades N, Landers T, Dolgalev I, Major JE, Wilson M, Socci ND, Lash AE, Heguy A, Eastham JA, Scher HI, Reuter VE, Scardino PT, Sander C, Sawyers CL, Gerald WL. Integrative genomic profiling of human prostate cancer. Cancer Cell. 2010; 18:11–22. [PubMed: 20579941]
18. Robinson D, Van Allen EM, Wu YM, Schultz N, Lonigro RJ, Mosquera JM, Montgomery B, Taplin ME, Pritchard CC, Attard G, Beltran H, Abida W, Bradley RK, Vinson J, Cao X, Vats P, Kunju LP, Hussain M, Feng FY, Tomlins SA, Cooney KA, Smith DC, Brennan C, Siddiqui J, Mehra R, Chen Y, Rathkopf DE, Morris MJ, Solomon SB, Durack JC, Reuter VE, Gopalan A, Gao J, Loda M, Lis RT, Bowden M, Balk SP, Gaviola G, Sougnez C, Gupta M, Yu EY, Mostaghel EA, Cheng HH, Mulcahy H, True LD, Plymate SR, Dvinge H, Ferraldeschi R, Flohr P, Miranda S, Zafeiriou Z, Tunariu N, Mateo J, Perez-Lopez R, Demichelis F, Robinson BD, Schiffman M, Nanus DM, Tagawa ST, Sigaras A, Eng KW, Elemento O, Sboner A, Heath EI, Scher HI, Pienta KJ, Kantoff P, de Bono JS, Rubin MA, Nelson PS, Garraway LA, Sawyers CL, Chinnaiyan AM. Integrative clinical genomics of advanced prostate cancer. Cell. 2015; 161:1215–1228. [PubMed: 26000489]
19. Karanika S, Karantanos T, Li L, Corn PG, Thompson TC. DNA damage response and prostate cancer: defects, regulation and therapeutic implications. Oncogene. 2014; 0
20. Ta HQ, Gioeli D. The convergence of DNA damage checkpoint pathways and androgen receptor signaling in prostate cancer. Endocrine-related cancer. 2014; 21:R395–407. [PubMed: 25096064]
21. Goodwin JF, Schiewer MJ, Dean JL, Schrecengost RS, de Leeuw R, Han S, Ma T, Den RB, Dicker AP, Feng FY, Knudsen KE. A Hormone-DNA Repair Circuit Governs the Response to Genotoxic Insult. Cancer Discov. 2013
22. Polkinghorn WR, Parker JS, Lee MX, Kass EM, Spratt DE, Iaquinta PJ, Arora VK, Yen WF, Cai L, Zheng D, Carver BS, Chen Y, Watson PA, Shah NP, Fujisawa S, Goglia AG, Gopalan A, Hieronymus H, Wongvipat J, Scardino PT, Zelefsky MJ, Jasin M, Chaudhuri J, Powell SN, Sawyers CL. Androgen receptor signaling regulates DNA repair in prostate cancers. Cancer Discov. 2013
23. Khanna KK, Jackson SP. DNA double-strand breaks: signaling, repair and the cancer connection. Nat Genet. 2001; 27:247–254. [PubMed: 11242102]
24. Suwaki N, Klare K, Tarsounas M. RAD51 paralogs: roles in DNA damage signalling, recombinational repair and tumorigenesis. Seminars in cell & developmental biology. 2011; 22:898–905. [PubMed: 21821141]
25. Liu C, Srihari S, Cao KA, Chenevix-Trench G, Simpson PT, Ragan MA, Khanna KK. A fine-scale dissection of the DNA double-strand break repair machinery and its implications for breast cancer therapy. Nucleic acids research. 2014; 42:6106–6127. [PubMed: 24792170]

26. Prakash R, Zhang Y, Feng W, Jasin M. Homologous Recombination and Human Health: The Roles of BRCA1, BRCA2, and Associated Proteins. Cold Spring Harbor perspectives in biology. 2015; 7
27. Slinker BK. The statistics of synergism. Journal of molecular and cellular cardiology. 1998; 30:723–731. [PubMed: 9602421]
28. Bliss C. The toxicity of poisons appled jointly. Ann. Appl. Biol. 1939:585–604.
29. Willers H, Gheorghiu L, Liu Q, Efstathiou JA, Wirth LJ, Krause M, von Neubeck C. DNA Damage Response Assessments in Human Tumor Samples Provide Functional Biomarkers of Radiosensitivity. Seminars in radiation oncology. 2015; 25:237–250. [PubMed: 26384272]
30. Talarico C, Dattilo V, D'Antona L, Menniti M, Bianco C, Ortuso F, Alcaro S, Schenone S, Perrotti N, Amato R. SGK1, the New Player in the Game of Resistance: Chemo-Radio Molecular Target and Strategy for Inhibition. Cellular physiology and biochemistry : international journal of experimental cellular physiology, biochemistry, and pharmacology. 2016; 39:1863–1876.
31. Castel P, Scaltriti M. The emerging role of serum/glucocorticoid-regulated kinases in cancer. Cell cycle. 2016:1–2.
32. Lowe JM, Nguyen TA, Grimm SA, Gabor KA, Peddada SD, Li L, Anderson CW, Resnick MA, Menendez D, Fessler MB. The novel p53 target TNFAIP8 variant 2 is increased in cancer and offsets p53-dependent tumor suppression. Cell death and differentiation. 2016
33. Liu T, Gao H, Yang M, Zhao T, Liu Y, Lou G. Correlation of TNFAIP8 overexpression with the proliferation, metastasis, and disease-free survival in endometrial cancer. Tumour biology : the journal of the International Society for Oncodevelopmental Biology and Medicine. 2014; 35:5805–5814. [PubMed: 24590269]
34. Day TF, Mewani RR, Starr J, Li X, Chakravarty D, Ressom H, Zou X, Eidelman O, Pollard HB, Srivastava M, Kasid UN. Transcriptome and Proteome Analyses of TNFAIP8 Knockdown Cancer Cells Reveal New Insights into Molecular Determinants of Cell Survival and Tumor Progression. Methods in molecular biology. 2017; 1513:83–100. [PubMed: 27807832]
35. Polkinghorn WR, Parker JS, Lee MX, Kass EM, Spratt DE, Iaquinta PJ, Arora VK, Yen WF, Cai L, Zheng D, Carver BS, Chen Y, Watson PA, Shah NP, Fujisawa S, Goglia AG, Gopalan A, Hieronymus H, Wongvipat J, Scardino PT, Zelefsky MJ, Jasin M, Chaudhuri J, Powell SN, Sawyers CL. Androgen receptor signaling regulates DNA repair in prostate cancers. Cancer Discov. 2013; 3:1245–1253. [PubMed: 24027196]
36. Plummer R. Poly(ADP-ribose)polymerase (PARP) inhibitors: from bench to bedside. Clinical oncology. 2014; 26:250–256. [PubMed: 24602564]
37. Ratner ES, Sartorelli AC, Lin ZP. Poly (ADP-ribose) polymerase inhibitors: on the horizon of tailored and personalized therapies for epithelial ovarian cancer. Current opinion in oncology. 2012; 24:564–571. [PubMed: 22759740]
38. Brenner JC, Ateeq B, Li Y, Yocum AK, Cao Q, Asangani IA, Patel S, Wang X, Liang H, Yu J, Palanisamy N, Siddiqui J, Yan W, Cao X, Mehra R, Sabolch A, Basrur V, Lonigro RJ, Yang J, Tomlins SA, Maher CA, Elenitoba-Johnson KS, Hussain M, Navone NM, Pienta KJ, Varambally S, Feng FY, Chinnaiyan AM. Mechanistic rationale for inhibition of poly(ADP-ribose) polymerase in ETS gene fusion-positive prostate cancer. Cancer Cell. 2011; 19:664–678. [PubMed: 21575865]
39. Lee JM, Ledermann JA, Kohn EC. PARP Inhibitors for BRCA1/2 mutation-associated and BRCA-like malignancies. Annals of oncology : official journal of the European Society for Medical Oncology / ESMO. 2014; 25:32–40.
40. Tangutoori S, Baldwin P, Sridhar S. PARP inhibitors: A new era of targeted therapy. Maturitas. 2015; 81:5–9. [PubMed: 25708226]
41. Aparicio A, Tzelepi V, Araujo JC, Guo CC, Liang S, Troncoso P, Logothetis CJ, Navone NM, Maity SN. Neuroendocrine prostate cancer xenografts with large-cell and small-cell features derived from a single patient's tumor: morphological, immunohistochemical, and gene expression profiles. The Prostate. 2011; 71:846–856. [PubMed: 21456067]

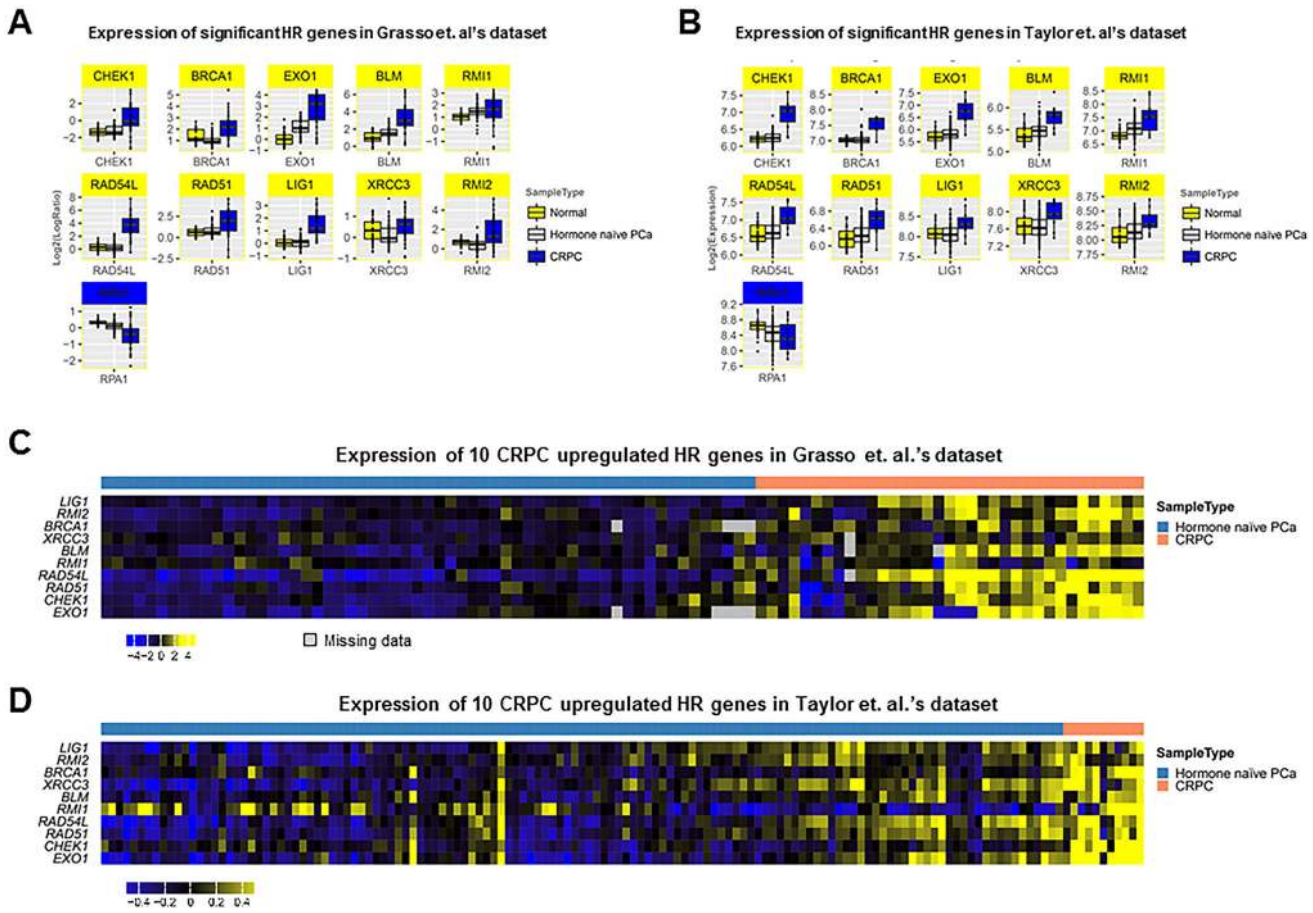

Fig. 1. HR gene expression in human normal prostate, primary PCa and CRPC tissue samples

(**A-B**) Boxplots showing 10 CRPC-upregulated (yellow) and 1 CRPC-downregulated (*RPA1*, blue) HR genes common to two published CRPC datasets. (**C-D**) Heatmaps showing expression of 10 common upregulated HR genes in two published CRPC datasets.

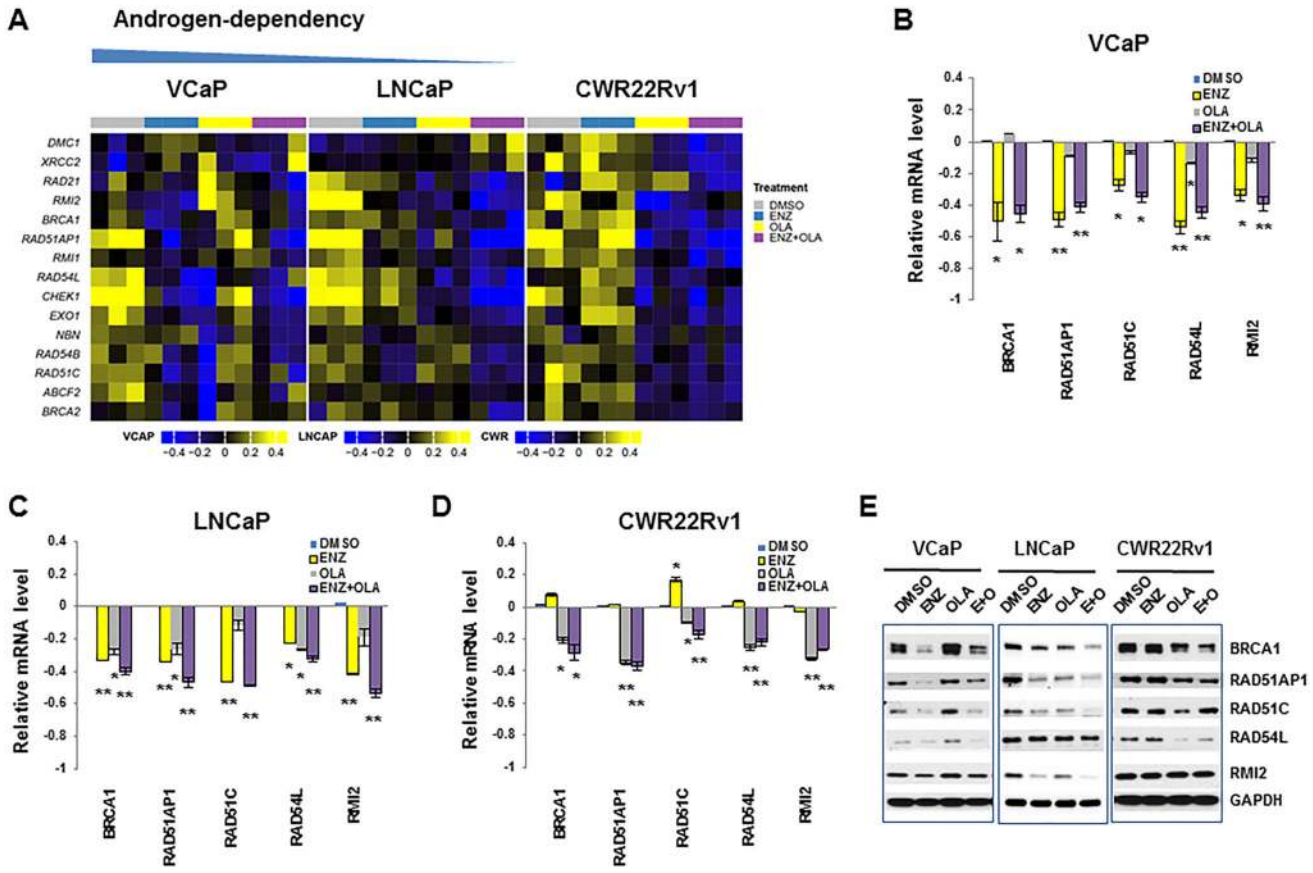

Fig. 2. Cell context-dependent ENZ and OLA downregulation of HR genes in PCa cells with different androgen dependency

(A) Heat map showing the expression of 15 HR-associated genes that were significantly altered by ENZ in AR-positive and androgen-dependent VCaP and LNCaP cells and in AR-positive, androgen-independent CWR22Rv1 cells. Significance (p<0.05) determined by Benjamini–Hochberg correction for multiple hypotheses testing. (**B-D**) qRT-PCR analysis of mRNA expression of five select HR genes in VCaP (B), LNCaP (C), and CWR22Rv1 (D) cells. Data are mean ± SD from three experiments. * p< 0.05, ** p<0.01 (Wilcoxon-Mann-Whitney test). (**E**) Western blotting analysis of five selected HR proteins in the indicated cell lines. Blots are representative of three or more experiments.

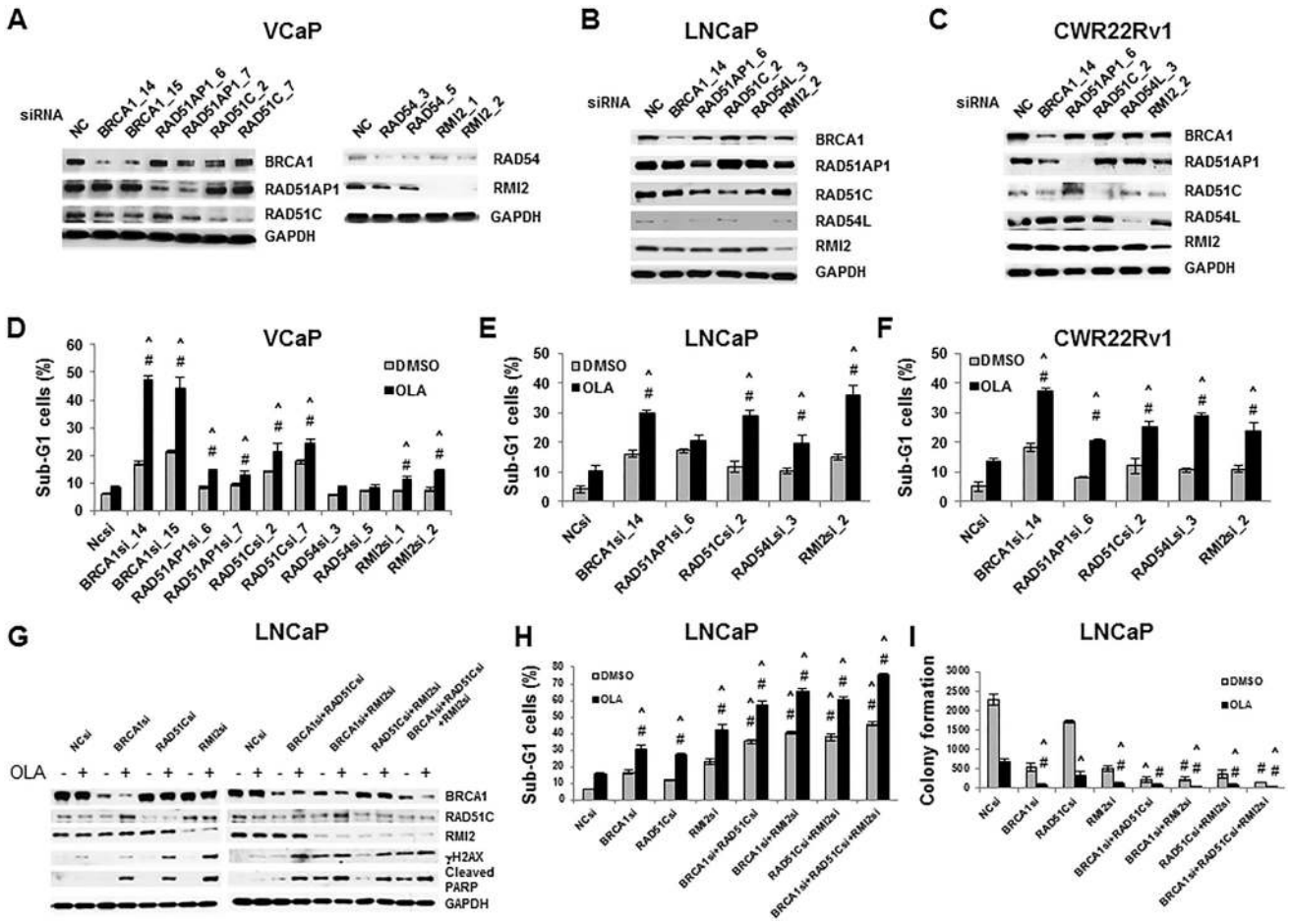

Fig. 3. HR gene silencing synergizes with OLA to increase cytotoxicity to PCa cells

(**A-C**) Western blotting analysis for the expression of HR genes in VCaP (A), LNCaP (B), and CWR22Rv1 (C) cells transfected with specific HR gene siRNAs (20 nM). Two siRNAs per HR gene were tested in VCaP cells, as indicated; one each was used in LNCaP and CWR22Rv1. Blots are representative of three or more experiments (**D-F**) Flow cytometry analysis of sub-G1 cells after siRNA and OLA treatment in VCaP (D), LNCaP (E), and CWR22Rv1 (F) cells transfected as in (A) 24 hours before treatment with DMSO or olaparib (OLA; 10 μM for 48 hours). (**G**) Western blotting analysis for BRCA1, RAD51C and RMI2 proteins, γH2AX abundance, and cleaved PARP abundance by RNA interference and OLA, as indicated, in LNCaP cells. Blots are representative of three or more experiments (**H**) Flow cytometry analysis of sub-G1 cells for synergistic effects of combinations of three selected HR gene siRNAs in the absence and presence of OLA in LNCaP cells. Data are means ± SD from three experiments. (**I**) Colony assay for synergistic effects of combinations of three selected HR gene siRNAs in the absence and presence of OLA in LNCaP cells. Data areas mean ± SD from three experiments. # synergy by two-way ANOVA; ^ synergy by Bliss Independent Analysis (table S1).

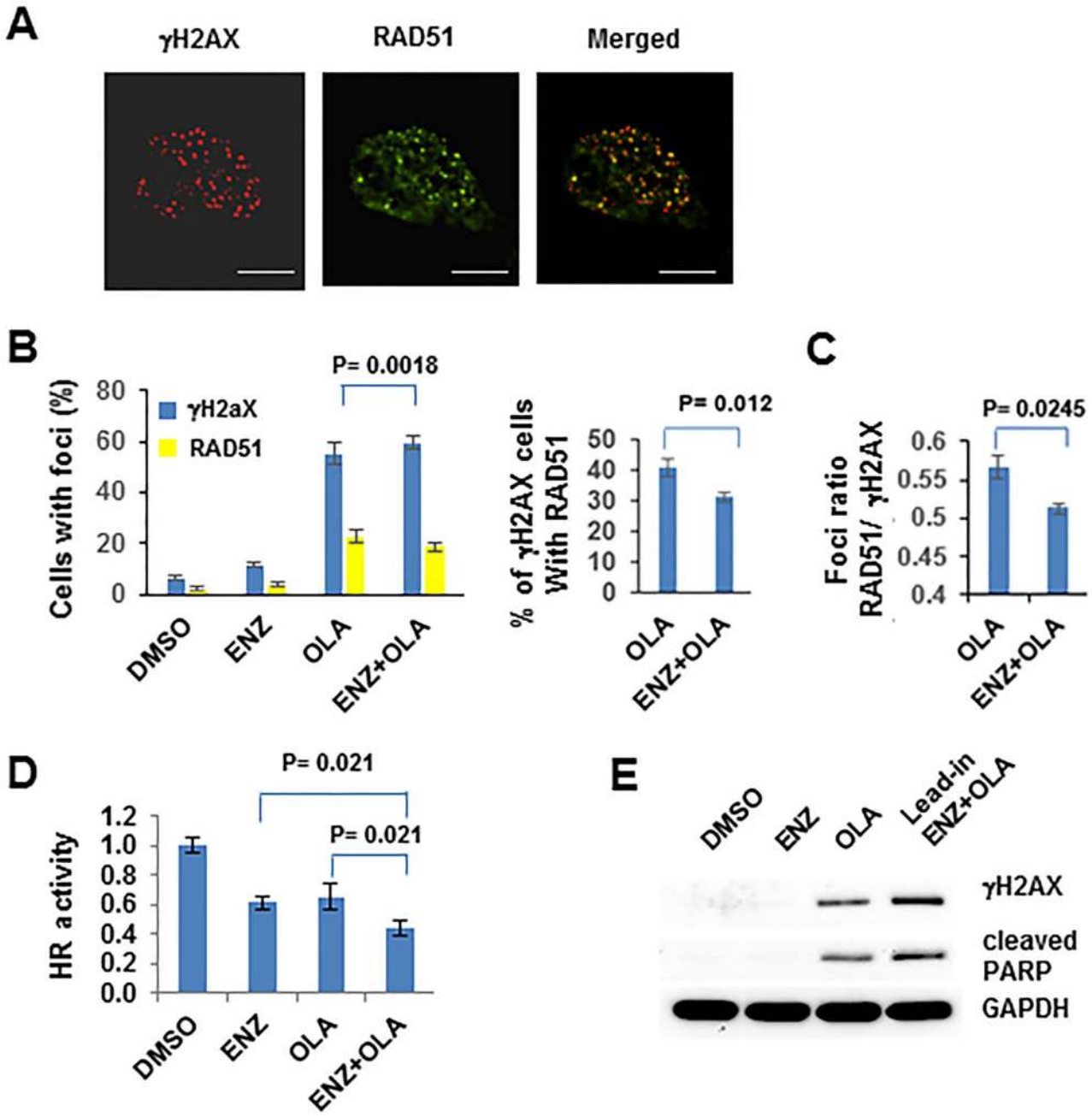

Fig. 4. ENZ and OLA suppress DNA repair in PCa

(A) Double immunofluorescence to detect γH2AX (red) and RAD51 (green) foci and their colocalization in OLA+ENZ treated LNCaP cells. (**B-C**) Quantitation (percentage)_of γH2AX foci-positive and γH2AX- and RAD51 focipositive cells (B) and the ration of of RAD51 to γH2AX foci in LNCaP cells. **(D)** Relative HR activity was calculated by a two-step normalization: the number of PCR cycles in assay primer group was normalized by that in universal primer group (internal control); the number of PCR cycles in treatment groups was normalized by that of control, with control=1. Data are means ± SDfrom three experiments. *P* values were derived from Wilcoxon-Mann-Whitney Test. **(E)** Western

blotting analysis of γH2AX and cleaved PARP in lead-in ENZ+OLA treated cells compared to those in OLA treated cells. Blots are representative of three experiments.

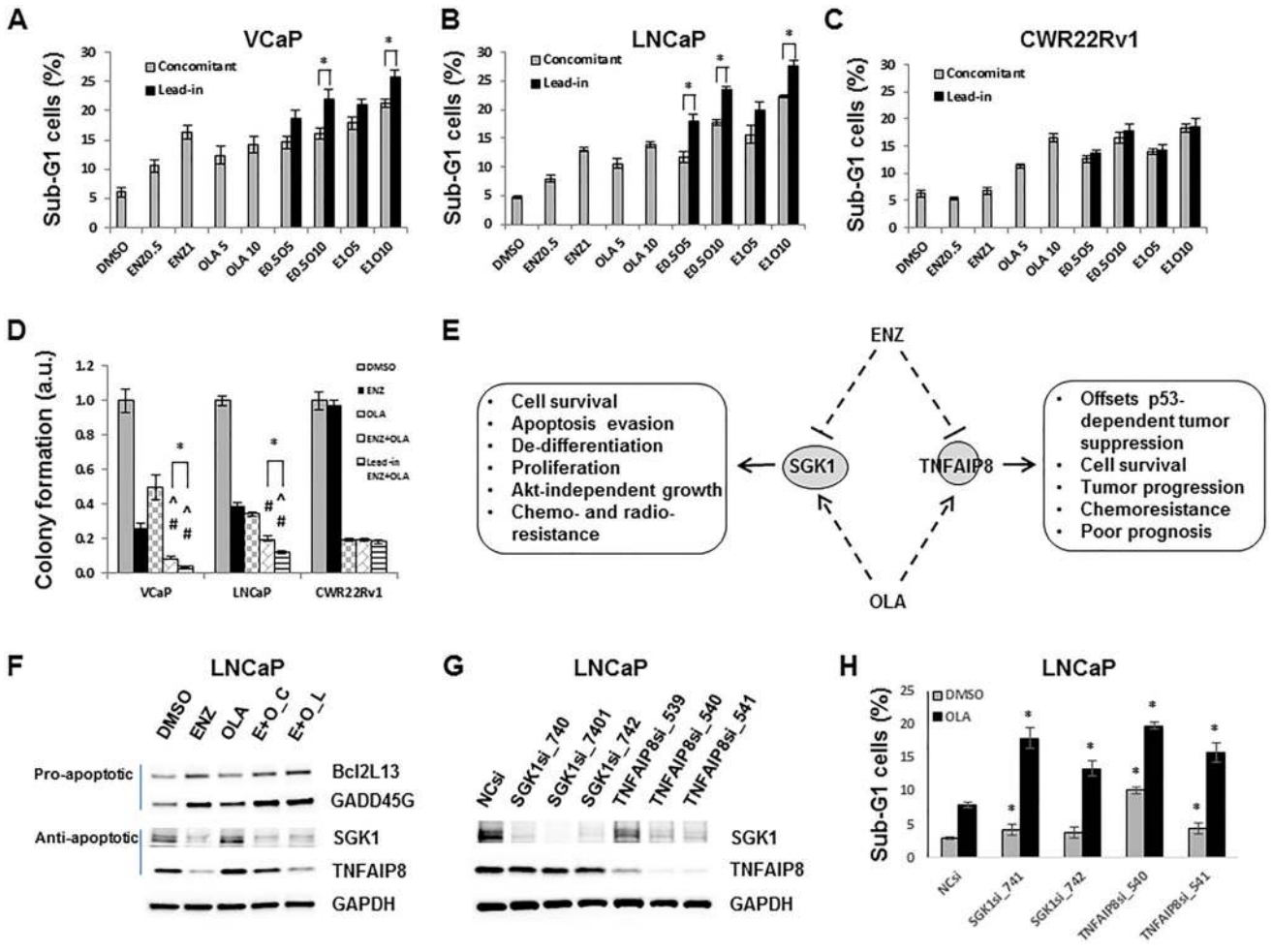

Fig. 5. A superior lead-in effect and its underlying mechanisms

(A-C) Cell cycle analysis. Cells were pretreated with ENZ (0.5 or 1 μM) or DMSO (vehicle control) for 24 hours, followed by the treatment with DMSO, or ENZ (0.5 or 1 μM) or OLA (5 or10 μM), or ENZ+OLA for 48 hours. **(D)** Colony assay. Optimal concentrations of ENZ and OLA were determined for each cell line by drug titration (fig. S2). Cells were pretreated with ENZ (VCaP, 100 nM; LNCaP, 150 nM; CWR22Rv, 1 μM) or DMSO (VH) for 24 hours, followed by treatment with ENZ, OLA (VCaP, 2.5 μM; LNCaP, 1.5 μM; CWR22Rv1, 500 nM), ENZ+OLA, or DMSO for 10–20 days depending on the cell line. # synergy by two-way ANOVA; ^ synergy by Bliss independence. **(E)** Functional illustration of two ENZ-downregulated and OLA-upregulated anti-apoptotic genes *SGK1* and *TNFAIP8*. **(F)** Western blotting analysis of selected pro- and anti-apoptotic proteins from LNCaP cells treated with DMSO, ENZ, OLA, E+O_C (concomitant) or E+O_L (lead-in). **(G)** Western blotting analysis for SGK1 and TNFAIP8 in control and siRNA-transfected LNCaP cells. Blots are representative of three experiments. **(H)** Sub-G1 cell analysis in control, SGK1 siRNA- or TNFAIP8 siRNA-transfected in LNCaP cells. Data are mean ± SD from three experiment. * $p<0.05$ by Wilcoxon-Mann Whitney test (A-C, vs the corresponding concomitant condition; H, vs the control siRNA with DMSO condition).

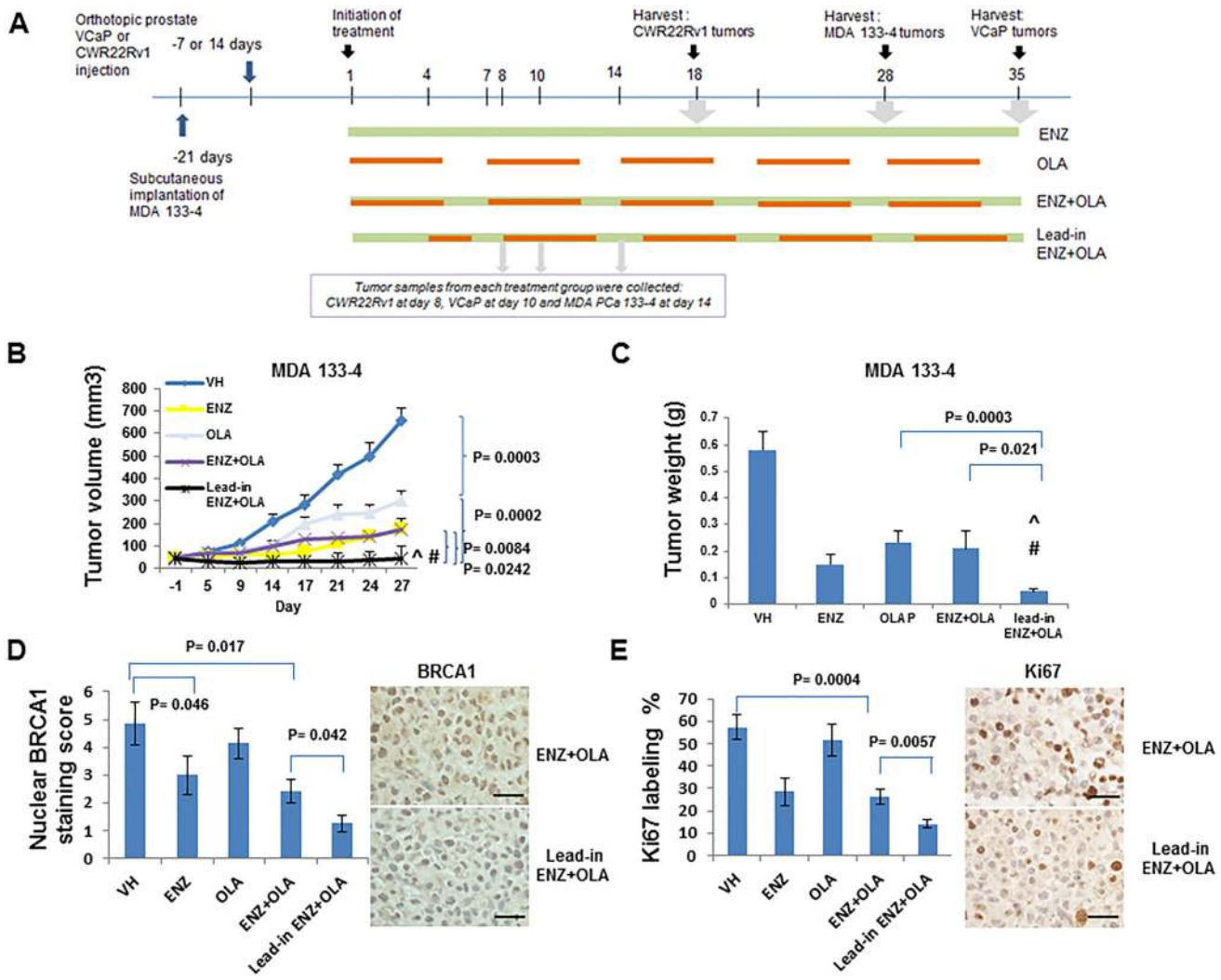

Fig. 6. Scheme of in vivo experiments and results of MDA PCa 133-4 subcutaneous model

(A) Scheme of in vivo experiments for VCaP and CWR22Rv1 orthotopic models and MDA 133- 4 subcutaneous model. (**B and C**). Suppression of MDA PCa 133-4 subcutaneous tumor growth by ENZ and OLA. Tumor growth (B) assessed 1 day before through 27 days of therapy and tumor weight (C) assessed at treatment day 27 in MDA 133-4 subcutaneous xenografts. Data are mean ± SE from 10 or more mice in each group. P-values derived from ANOVA t-test. # indicates synergy determined by two-way ANOVA; ^ indicates synergy determined by Bliss Independent Analysis. (**D and E**) Immunostaining for BRCA1 (D) and Ki67 (E) at day 14 of the indicated treatment. Data are mean ± SE from XXX7 or more mice; P values were derived from Wilcoxon-Mann-Whitney Test.

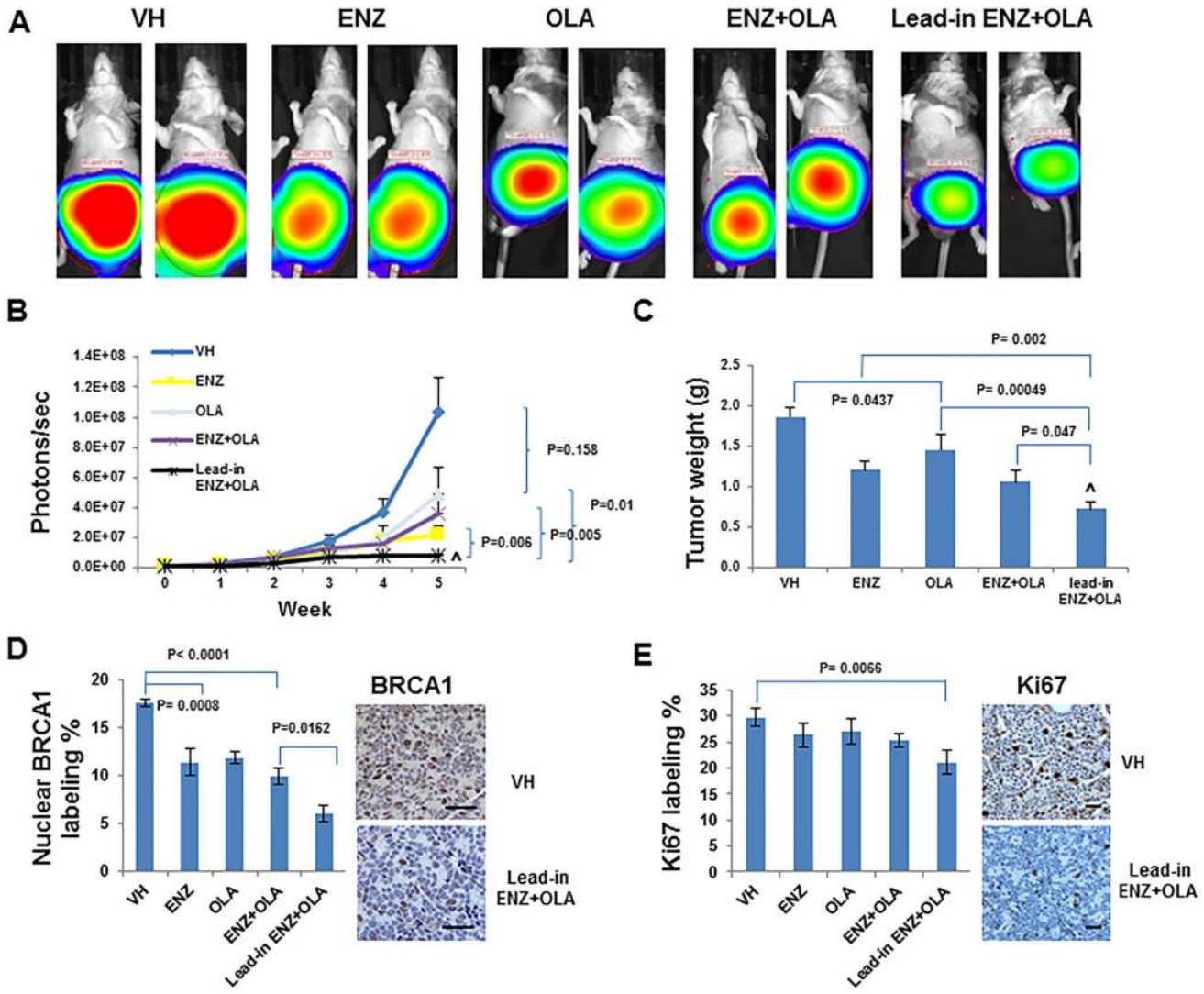

Fig. 7. Suppression of VCaP orthotopic xenograft tumor growth by ENZ and OLA treatment

(**A to C**) Representative luminescent images (A), tumor growth (B), and tumor weight (C) of VCaP orthotopic xenografts treated as indicated. Images are representative and data are mean ± SE from 17 or more mice in each group. P-values are derived from ANOVA t-test. ^ indicates synergy determined by Bliss Independent Analysis. **(D and E)** Immunohistochemcal staining for BRCA1 (D) and Ki-67 (E) at 7 (BRCA1) or 10 (Ki-67) days of the indicated treatment. Data are mean ± SD from 4 or more mice. *P* values were derived from Wilcoxon-Mann-Whitney Test.

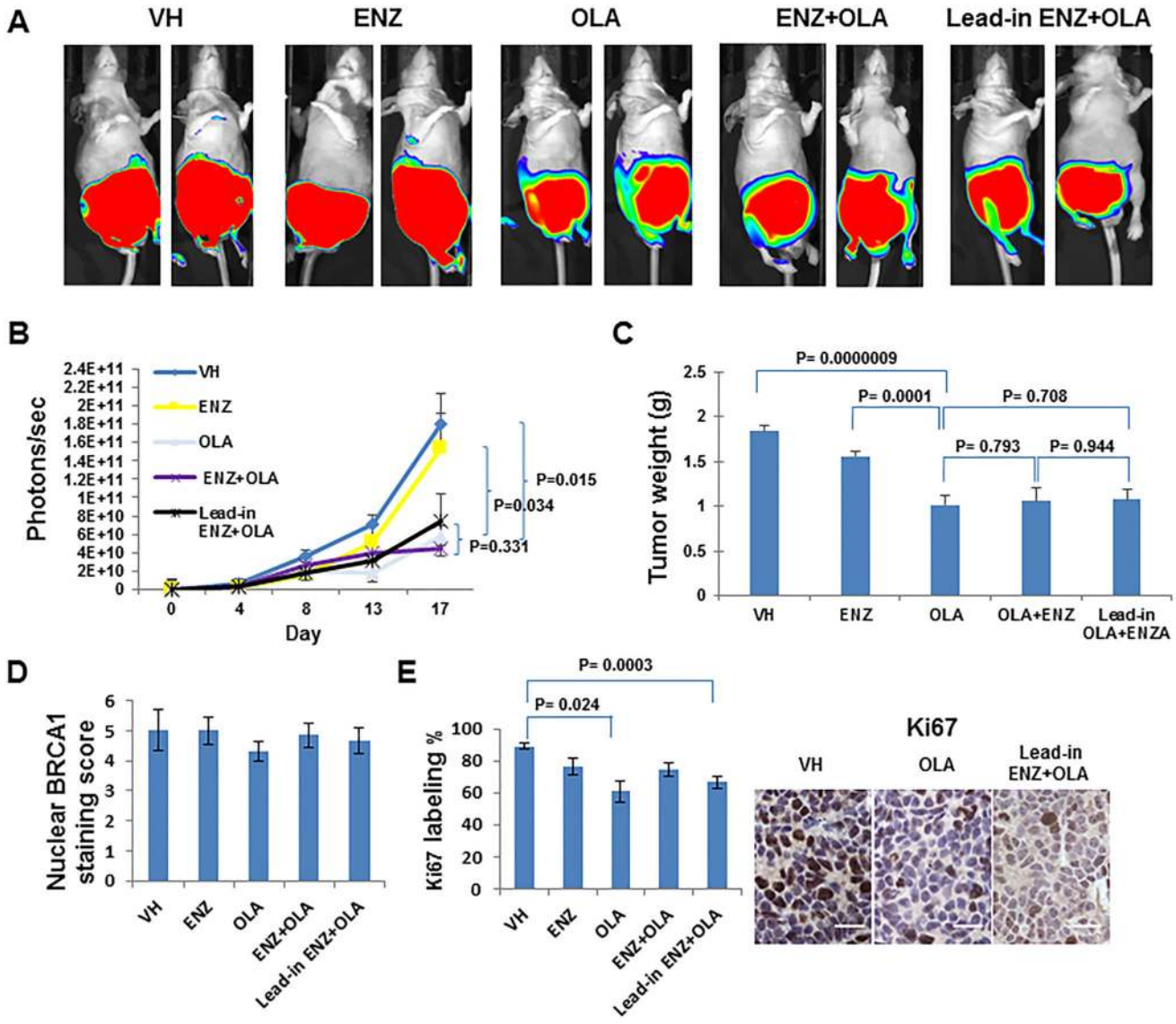

Fig. 8. Suppression of CWR22Rv1 orthotopic xenograft tumor growth by ENZ and OLA treatment

(**A**) Representative bioluminescent images from 10 or more mice in each group. (**B and C**) Tumor growth (B) and weight (C) of CWR22Rv1 orthotopic xenografts from mice treated as indicated. Data are mean ± standard error. ^ synergy by Bliss Independent Analysis. **(D and E)** Immunohistochemical staining for BRCA1 (D) and Ki-67 (E) in tumors removed from mice after 8 days of the indicated treatment. Data are mean ± standard error from 6 or more mice. *P* values were derived from Wilcoxon-Mann-Whitney Test.